PCCP

Accepted Manuscript

ROYAL SOCIETY OF CHEMISTRY

www.rsc.org/pccp

Physical Chemistry Chemical Physics RSCPublishing

ARTICLE

Mechanism of Pd-catalyzed Formation of Coumarin. A Theoretical Study.

Cite this: DOI: 10.1039/x0xx00000x

Received 00th January 2012,
Accepted 00th January 2012

DOI: 10.1039/x0xx00000x

www.rsc.org/

S. Nedd[a] and A. N. Alexandrova*[a,b]

The mechanism of formation of coumarin via the Pd-catalyzed intramolecular hydroarylation of the C-C triple bond is elucidated computationally, in corroboration with experimental data. It is shown that the reaction follows the concerted metalation-deprotonation (CMD) mechanism. The typically suspected mechanisms of ambiphilic metal ligand activation (AMLA), electrophilic aromatic substitution (EAS), and oxidative addition (OA) are suggested to be non-competitive, based on predicted conformations and energetics. Two forms of the Pd catalysts are used: $Pd(OAc)_2$, and $Pd(TFA)_2$. The predicted activation free energy barrier for the TFA-based catalyst is lower, both in the gas phase and in the CH_2Cl_2 solvent, in agreement with the experimental observations. Adding electron-withdrawing groups to the catalyst assists the first and rate-limiting step of the reaction, deprotonation of the aromatic ring, as understood through charge analysis.

Introduction

Catalytic activation of aromatic C-H bonds, which may be directed to new and useful reactions including C-C bond formations, remains a long-term challenge to chemists,[1-3] and it is of considerable interest for the chemical and pharmaceutical industries.[4-8] Of a particular note are coumarins (Fig. 1.1) and also quinolinones, which have many applications as novel therapeutic agents and prompt the development of general and efficient methods for their preparation.[9-18] For example, coumarin derivatives such as furocoumarins show many biological (photobiological activity in particular) and industrial applications.[19] Thus, there is great need for the identification and confirmation of feasible mechanisms and catalysts for the efficient production of these compounds.

The efficient intermolecular and intramolecular hydroarylation of C-C triple bonds in the presence of Pd and Pt catalysts by simple arenes (according to equation 1) has already been reported towards the formation of coumarins via experiment.[19,20]

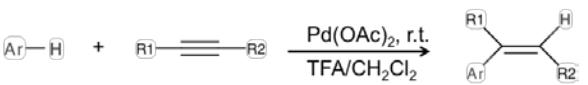

(1)

The production of coumarins and quinolinones according to this reaction starts from the typical precursors shown in Fig. 1.2. When X = O and R = H in Fig. 1.2, the result is the vanilla version of coumarin precursor. The catalyzed reaction of the formation of coumarin from this vanilla precursor is schematically shown in Fig. 1.3, and it is the subject of the present study. It has been indicated[20] that the palladium(II) acetate ($Pd(OAc)_2$) catalyst gives 90% yield in the reaction of catalyzed cyclization of 4'-tert-butylphenyl phenylpropiolate to form the coumarin analog, 4-phenyl-6-tert-butylcoumarin. In this reaction, the intramolecular coordination of the aryl carbon and the ethynyl group by the palladium catalyst was

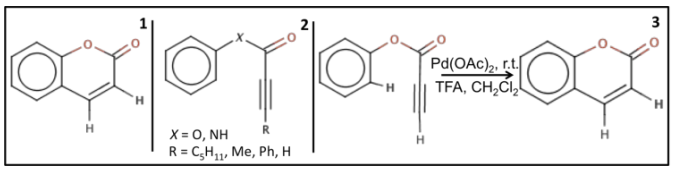

Figure 1. (1) The general structure of coumarin, (2) selected quinolinones and coumarin precursor derivatives, and (3) the reaction of the coumarin formation from the vanilla precursor, phenylpropriolate, used in this study.

exploited, giving yields greater than those based on the intermolecular mechanisms. The catalytic alkyne hydroarylation in C-H activation mechanism was suggested for this intramolecular coordinated system. However, a follow up paper indicated from experiment that the electrophilic aromatic substitution (EAS) mechanism may be preferred.[21] Thus, the mechanism in the production of coumarin is unsubstantiated where several potential mechanisms have been identified. It is noted that the rate of reaction is increased with the addition of the electron-withdrawing group, trifluoroacetate (TFA), to the catalyst, in dichloromethane. In this paper, the mechanism of this Pd-catalyzed reaction (Fig. 1.3), and the effect of adding TFA to the Pd(II) catalyst ($Pd(TFA)_2$) are explicated. First, however, the four potential mechanisms are introduced in some detail.

In Fig. 2, the two possible coordination forms for the Pd(II) catalysts to the studied substrate are depicted. These two possible coordinations are due to *cis*-addition and *trans*-addition of Pd(II), which form the necessary starting points in the mechanisms studied. *Cis*-addition is the Pd(II) coordination to the triple C-C bond and aryl C-H bond, as shown in Fig. 2 in panel 1. *Trans*-addition is the Pd(II) coordination to the triple C-C bond in the *trans* position relative to the aryl C-H bond, as shown in Fig 2, in panel 2.

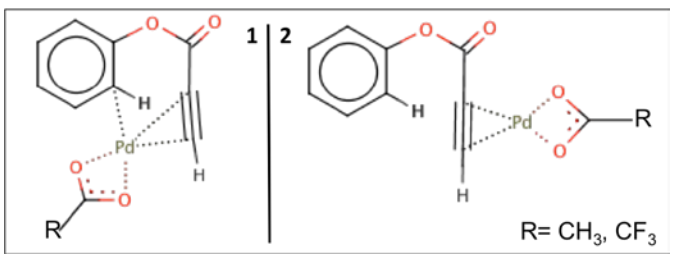

Figure 2. Schematic representation of Pd(II) catalyst bound to the reactants in the EAS production of coumarin. The cationic forms of the catalysts, $Pd(OAc)^+$ (R=CH_3), and $Pd(TFA)^+$,(R=CF_3) are shown. Panel 1 shows the *cis*-addition, and panel 2 shows the *trans*-addition typically used in the literature.

Electrophilic aromatic substitution mechanism. EAS catalyzed by Pd(II) has been cited as the possible mechanism for coumarin production.[21] The EAS mechanism consists of four primary parts: (1) alkyne coordination to Pd(II) via *trans*-addition, (2) nucleophilic attack by the aryl C-H on the ethynyl group forming a Wheland intermediate (ring closure occurs, however the aryl hydrogen shown in bold in Fig. 2 is uncleaved), (3) protic cleavage of the aryl hydrogen, and (4) protonolysis of the resulting Pd-vinyl complex.[21] In this paper, only part 1 of the EAS mechanism is studied, because it is sufficient in assessing the feasibility of this mechanism. It is connected to how energetically feasible the two addition forms are.

Oxidative addition mechanism. The OA mechanism outlined in Fig. 3 is a commonly used mechanism for the insertion of low valence transition metals.[3,22] In the intramolecular hydroarylation reaction of formation of coumarin, this metal insertion involves the cleavage of the aryl C-H bond by attaching a Pd(II) catalyst to phenylpropiolate (**oNC** to **oC**, Fig. 3), followed by a six-membered ring closure and then the attachment of a hydrogen to the ethynyl group, toward the products, **oRP**.

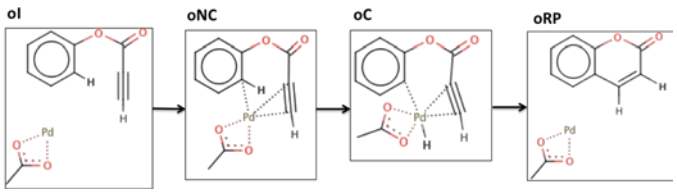

Figure 3. Schematic representation of the OA mechanism using the cationic $Pd(OAc)^+$ catalyst as an example. The mechanism for $Pd(TFA)^+$ is analogous. The labels represent the different states of the systems, including the separated Pd catalyst and phenylpropiolate (oI), starting complex (oNC), cleaved aryl C-H (oC), and separated Pd catalyst from coumarin product (oRP).

Concerted metalation-deprotonation mechanism. The CMD pathway is signified by the cleavage of an aryl C-H by a metal catalyst with the assistance of a base.[23] There is already support for this mechanism borne out by Kinetic Isotope Effect (KIE) data, which suggests that this mechanism may be the most probable option in the production of coumarin.[23,24] The CMD mechanism in the formation of coumarin is shown in Fig. 4, for the $Pd(OAc)_2$ catalyst, with the stationary points shown in the following order: non-bound $Pd(OAc)_2$ and phenylpropriolate (**cI**), minima of bound $Pd(OAc)_2$ and phenylpropriolate with non-cleaved aryl C-H (**cNC**), intermediate formed upon cleavage of the aryl C-H bond (**cC**), intermediate where the coumarin product is still bound to the $Pd(OAc)_2$ catalyst (**cP**), and the final state corresponding to the unbound $Pd(OAc)_2$ and coumarin product (**cRP**). The same terms are used for the $Pd(TFA)_2$ catalyst. Again, a pinnacle aspect of this CMD reaction mechanism is the usage of the acetate as a base in order to assist in the removal of the hydrogen from the aryl C-H; the usage of this acetate has been suggested to be necessary for the feasibility of the process.[25] There is already some evidence in previous CMD-related papers that indicate that the typically considered alternative oxidative addition mechanism offers an intermediate that is too high in energy, and would not be the most feasible mechanism.[26,27]

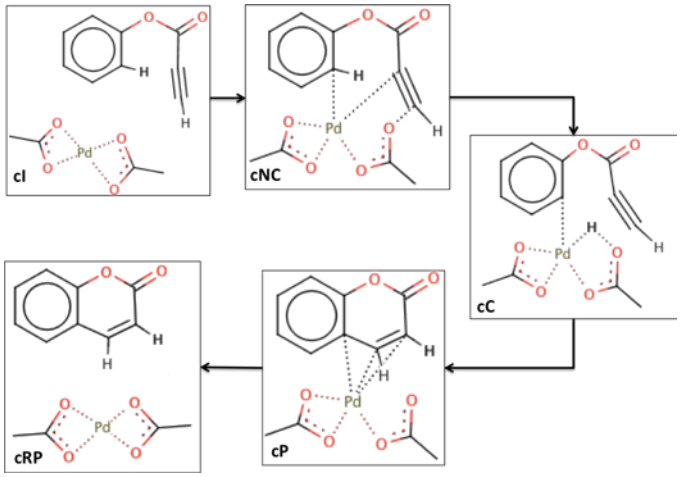

Figure 4. Schematic representation of the CMD mechanism for the palladium-catalyzed intramolecular hydroarylation forming coumarin. The system labels, which represent the various CMD model systems, are: **cI** - non-bound $Pd(OAc)_2$ and phenylpropriolate, **cNC** - bound $Pd(OAc)_2$ and phenylpropriolate with non-cleaved aryl C-H, **cC** - cleaved aryl C-H intermediate, **cP** - Coumarin product with attached $Pd(OAc)_2$ catalyst, **cRP** - removed coumarin product.

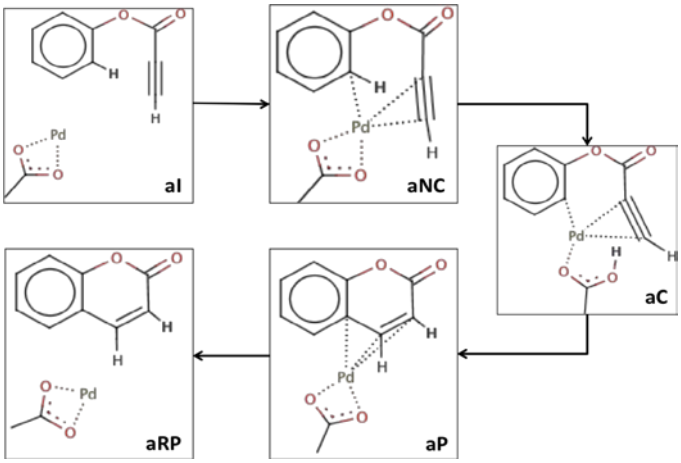

Figure 5. Schematic representation the AMLA mechanism for the palladium-catalyzed intramolecular hydroarylation forming coumarin. The system labels are: **aI** - non-bound $Pd(OAc)^+$ and phenylpropriolate, **aNC** - bound $Pd(OAc)^+$ and phenylpropriolate with non-cleaved aryl C-H, **aC** - cleaved aryl C-H, **aP** - Coumarin product with attached $Pd(OAc)^+$ catalyst, **aRP** - removed coumarin product.

Ambiphilic metal ligand activation. The AMLA mechanism[28,29] is similar to the CMD mechanism in that it is also signified by the cleavage of an aryl C-H by a metal catalyst with the assistance of a base. However, for our system, the AMLA mechanism is represented by one acetate, $Pd(OAc)^+$ instead of $Pd(OAc)_2$. The AMLA mechanism is shown in Fig. 5, with the labels assigned as follows: non-bound $Pd(OAc)^+$ and phenylpropriolate (**aI**), the initial bound complex of $Pd(OAc)^+$ and phenylpropriolate with non-cleaved aryl C-H bond (**aNC**), intermediate corresponding to the cleaved aryl C-H (**aC**), the complex of the product with the catalyst $Pd(OAc)^+$ (**aP**), and finally the unbound product and restored $Pd(OAc)^+$ catalyst (**aRP**).

In this theoretical work, the four mechanisms of Pd-catalyzed formation of coumarin are studied: CMD, AMLA, EAS, and OA. There are limitations in the experimental approaches in the attempts to identify the correct mechanism.[20,21] The gas phase free energy profiles and condensed phase (dichloromethane) energy profiles for all mechanisms are computed here. We will show that the CMD mechanism is the most feasible one. It is also noted that these hydroarylation reactions have been shown to increase their yield upon the addition of electron withdrawing groups to the catalyst. As mentioned above, in the case of the intramolecular hydroarylation reaction, trifluoroacetate (TFA) was used[19,30,31] in dichloromethane as the solvent.

Thus, the effects of TFA and dichloromethane on the reaction free energy barrier will be elucidated as well. The analysis of the electronic structure will be presented to shed light on the effect of the electron withdrawing groups on the rate of the reaction.

Computational Details

All calculations were done using the TURBOMOLE[35] computational program package. Structural optimizations and vibrational frequency calculations were done at the level of theory of RI-TPSS/def2-SVP level of theory, where the Pd metal was treated with RI-TPSS and the effective core potential basis set, def2-TZVPP.[33] TPSS is a nonempirical meta-generalised gradient approximation functional and is a commonly used functional that gives a high quality description of various systems including Pd systems.[39,40,41] The combination of def2-SVP for all atoms (def2-TZVPP for Pd) in the Pd systems defined in this work, is considered quantitative. The usage of the def2 basis sets, requires the use of ECPs for atoms in the range of Rb-Rn.[42] These ECPs have been rigorously optimized to ensure accurate and faster calculations and values relative to the analogous all-electron basis set.[42] All intermediates were confirmed to be true minima, and all transitions states to be the first-order saddle points with the imaginary frequencies aligned with the reaction coordinate. RI-TPSS/ single point energy calculations were done for the optimised structures of the stationary points on the reaction profiles, and those energies were used in the construction of the free energy profiles of the reactions.[35-38] All density functional theory (DFT) calculations employed the Grimme's D3 correction, which further improves the quality of results obtained from the TPSS functional level of theory.[43] The transition state searches were the Linear Synchronous Transit, where at least ten structures were sampled between energy minima structures. Saddle point energy and structural relaxation calculations were done on these 10 structures, followed by a vibrational frequency analysis to confirm the presence of transition state. A charge distribution analysis was performed using the natural-population analysis (NPA) method.[44] In order to determine the solvent effects of CH_2Cl_2, single points total energies at zero Kelvin were performed using TURBOMOLE's version of the Conductor-like Screening Model (COSMO).[45] The dielectric constant for the dichloromethane solvent used was 8.93.[46,47] The coordinates for all stationary state structures are given in the Supporting Information.

Results and Discussion

All species along the four reaction profiles were found to be spin-singlets, with the exception of the **oC** species in Fig. 3 (the OA mechanism), which is a triplet. We do not explicitly calculate the state-crossing points on the OA reaction profiles, because it appears to be unnecessary. However, it is anticipated that for a metal like Pd, the spin-orbit coupling is significant to make state-crossing energetically-accessible. Cartesian coordinates of all stationary points on the reaction profile are given in the Supporting Information.

Electrophilic Aromatic Substitution. The EAS mechanism requires a *trans*-addition of the Pd(II) catalyst as shown in panel 2 in Fig. 2. The EAS mechanism has been suggested based on the experimental evidence coming from Kinetic Isotope Effect (KIE) analysis, calculated elsewhere.[21] The same reference concedes that Pd(II) catalysts prefers to bind in the *cis* form in general,[21] and it has been already shown that in most cases the *cis*-addition of the Pd(II) catalyst is preferred.[32,33] Thus, in order to clarify the plausibility of the EAS mechanism, the relative energies of the two forms of bound Pd(II) catalyst (the *cis*-addition form (panel 1 in Fig. 2) and the *trans*-addition form (panel 2 in Fig.2)) have been determined.

For the cationic $Pd(OAc)^+$ catalyst, the *cis*-addition form is the lower energy form by ΔG_{298K}=12.6 kcal/mol in the gas phase compared to the *trans*-addition form, whereas in dichloromethane solvent the *cis*-addition form is lower in energy by the ΔE_{0K}=15.1 kcal/mol. For the cationic $Pd(TFA)^+$ catalyst, structural optimizations revealed a rearrangement of the *trans*-addition form into the *cis*-addition form, indicating that *trans*-addition form is not a minimum, and solidifying the preference for *cis*-addition. Since the *trans*-addition form is required for the EAS mechanism, this simple set of structural relaxations indicates that formation of coumarin via the formation of the characteristic wheland intermediate of the EAS mechanism, most likely follows another pathway, initiated by the Pd(II) catalyst binding in the *cis*-addition form.[34]

Oxidative Addition Mechanism. For the alternative mechanism of OA, the calculated free energy (298K) reaction profiles in the gas phase and condensed (dichloromethane) phase are shown in Fig. 6. In the gas phase, for the cationic forms of both catalysts, $Pd(OAc)^+$ and $Pd(TFA)^+$, the lowest point on the free energy profile is $Pd(OAc)^+$ bound to phenylpropiolate (**oNC**). It is 14.8 kcal/mol lower than the final product of coumarin and unbound $Pd(OAc)^+$ (**oRP**) (24.3 kcal/mol lower for $Pd(TFA)^+$). The trends outlined in the gas phase free energy reaction profile change very little in dichloromethane as shown in parentheses in Fig. 6.. Both gas phase and solvent phase results suggest that the system will get trapped in the **oNC** intermediate, essentially terminating the OA mechanistic pathway. The energy span of this reaction is just too large. Furthermore, the problem is most apparent for the $Pd(TFA)^+$ catalyst in dichloromethane, and that disagrees with the effect of fluorination being beneficial for the catalysis.

The **oC** structure also has the cleaved hydrogen on the opposite side of the Pd(II). This suggests a high barrier to the formation of **oC** from o**NC** exists, and here it is estimated to be greater than 62.1 kcal/mol. The full search for the transition states on the OA reaction profiles was found unnecessary. From the presented considerations, the OA pathway is unlikely to be used in the formation of coumarin from phenylpropiolate.

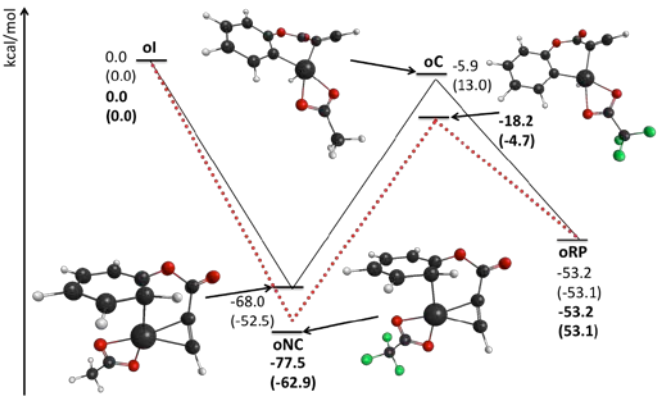

Figure 6. Gas Phase and condensed phase (dichloromethane) relative free energy (298K) profile diagram showing the OA mechanism in Pd-catalyzed intramolecular hydroarylation forming coumarin. The solid line represents the cationic $Pd(OAc)^+$ catalyst, and the bold dotted line represents the cationic $Pd(TFA)^+$ catalyst. Condensed phase (dichloromethane) relative total energy values are given in parentheses. The atom colours are black (C), white (N), red (O), and green (F); the large black atom (Pd).

Concerted metalation-deprotonation. For the CMD mechanism, in Fig. 7, the gas phase free energy (298K) and the condensed phase (dichloromethane) total energy (298K) reaction profiles are shown. Let us first focus on the gas phase results. The initial binding free energies, ΔG_{298K}, for the formation of **cNC** are 25.7 kcal/mol with $Pd(OAc)_2$, and 1.0 kcal/mol with $Pd(TFA)_2$). The rate-determining step in this reaction is the formation of the intermediate **cC** via the transition state, **c1TS** (Fig. 7). The corresponding free energy barrier is $\Delta G^{\ddagger}_{298K}$=25.3 kcal/mol with $Pd(OAc)_2$, and $\Delta G^{\ddagger}_{298K}$=13.9 kcal/mol with $Pd(TFA)_2$. Thus, the fluorination of the Pd(II) catalyst has a major effect of lowering the barrier height at standard conditions of room temperature and atmospheric pressure, in an agreement with the experiment. The barrier with $Pd(TFA)_2$ corresponds to the very reasonable turnover frequency of ~3600, which is based on the energy span approximation.[48] This TOF was also calculated for the OA mechanism, where the **oC** free energy was used to approximate the barrier height. In the OA mechanism the determination of the barrier height between **oNC** and **oC** (**o1TS**) involves an analysis of spin crossing states, which is beyond the scope of this paper, however, it is reasonable to suggest that the **oC** species would give close to the lowest possible value for the **o1TS** species. Hence, the TOF for OA is 4.37×10^{-19}, which is effectively 0. The TOF value for AMLA is discussed in a later section. The second low-energy transition state, **c2TS**, corresponds to the concerted ring closure and proton transfer. The forming intermediate, **cP**, then dissociates with a small barrier (in **c3TS**) to yield the final products, **cRP**. The relative free energy of the separated final coumarin product and the Pd(II) catalyst is ΔG_{298K}=-53.2 kcal/mol, indicating the highly exothermic character of the reaction, as expected.

The CMD reaction profiles in dichloromethane (bold numbers in parentheses in Fig. 7) are incomplete, however this condensed phase data suggests similar trends to those found in the gas phase. Also, all

of these condensed phase values are consistently lower than their gas phase counterpart in the CMD mechanism. Here, the initial binding energies for **cNC** were lower than those in the gas phase, for both catalysts. The reaction barrier heights are lowered to 22.1 kcal/mol for the $Pd(OAc)_2$ and to -3.7 kcal/mol for $Pd(TFA)_2$. The already published[20] experimental data suggests that the dichloromethane solvent aids in the increase in reaction rates. This should be replicated in our results via the reduction of the barrier heights, which is indeed observed. It is thus clear that via the reduction of the reaction barriers, the dichloromethane solvent is involved promoting a greater reaction rate in the CMD mechanism.

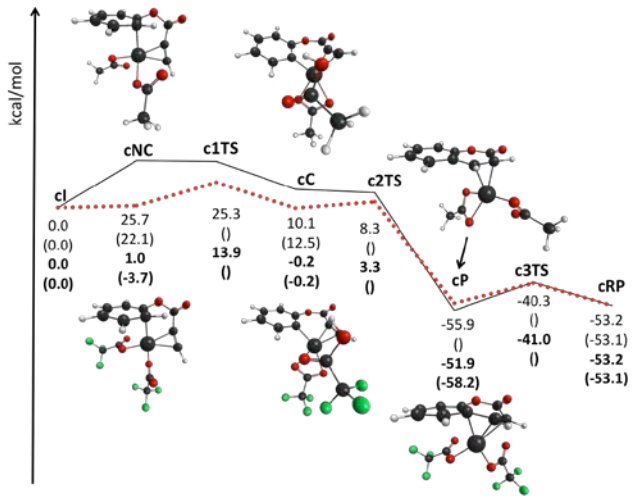

Figure 7. CMD reaction pathways with relative free energy values (298K) for the formation of coumarin in gas phase and dichloromethane. The solid line represents the $Pd(OAc)_2$ catalyst, and the bold dotted line and bold numbers represents $Pd(TFA)_2$. Condensed phase (dichloromethane) relative total energy values are given in parentheses. Units are kcal/mol. The zoomed-in structures of the optimised minima are (from left to right) NC, C, and P. The atom colours are black (C), white (N), red (O), and green (F); the large black atom (Pd). Due to problems associated with SCF convergence and vibrational analysis of COSMO job, there are several missing free energy values for the condensed phase (dichloromethane).

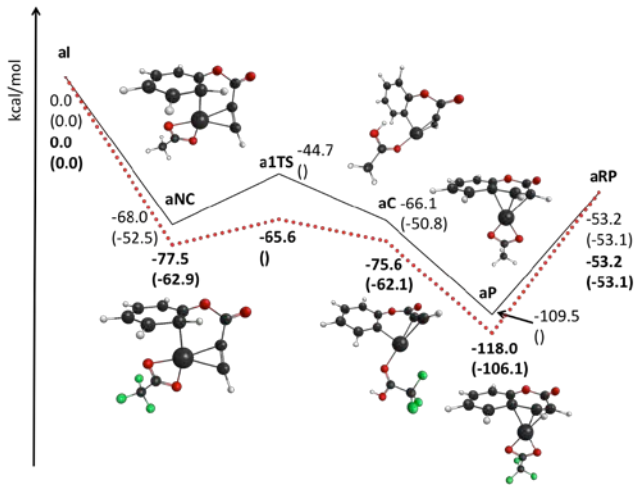

Figure 8. Gas Phase free energy (298K) profile diagram showing the ambiphilic metal ligand activation mechanism in palladium-catalyzed intramolecular hydroarylation forming coumarin. Condensed phase (dichloromethane) relative total energy values are given in parentheses. The solid line represents the cationic $Pd(OAc)^+$ catalyst, and the bold dotted line represents the cationic $Pd(TFA)^+$ catalyst. **aI**, **aNC**, **aC**, **aP**, and **aRP** refer to the structures indicated in Fig. 5. Units are kcal/mol. **a1TS** is the transition state between **aNC** and **aC**. The atom colours are black (C), white (N), red (O), and green (F); the large black atom (Pd).

Ambiphilic metal ligand activation. The AMLA mechanism is similar to the CMD mechanism. The results for AMLA are shown in Fig. 8. The gas phase and condensed phase (dichloromethane) free energy (298K) reaction profiles are shown. These reaction profiles have been limited to show primarily the barrier associated with **a1TS** (the transition state between **aNC** and **aC** from Fig. 5), which is analogous to the rate determining transition state identified in the CMD mechanism (**c1TS**). The stationary states for the coumarin product are also included.

From Fig. 8, AMLA looks unfeasible due to the trapping intermediate **aP**, which is 64.8 kcal/mol lower in energy than the final product, **aRP**.. Also, using the energy span approximation, AMLA has a turnover frequency of 3.73×10^{-44}, and like in the case of OA is effectively 0. It is also noted that condensed phase results are higher in energy, which suggests a destabilizing effect of the solvent, where the opposite should be true based on the mentioned experiment data[20]. These flaws are sufficient to discount the ALMA mechanism; it is evident that another base must be involved, as is the case in the CMD mechanism.

On the effect of catalyst fluorination and solvation. Based on the presented results, the CMD mechanism is the most likely one for the formation of coumarin. It has the most feasible energetics, and it is the only mechanism that fully agrees with the experiment in the predicted effect of solvation and catalyst fluorination. In order to explicate these effects further, we focus on the cleaved aryl C-H intermediate (**cC**), which immediately follows the rate-limiting transition state in the CMD mechanism. The geometric and electronic structures of **cC** for the two catalysts are analyzed in order to shed light on the benefit of having the electron-withdrawing group, TFA, on the catalyst for this reaction.

Fig. 9 presents several characteristic bond lengths and atomic charges for intermediate **cC**. One thing to notice is the dramatic difference in the distance between the phenyl ring and the abstracted hydrogen attached to acetate group of the Pd(II) catalyst. Furthermore, the acidity of the abstracted hydrogen attached to the carboxyl group is lower in the case of $Pd(TFA)_2$, as assessed from the dipole moment of the formed O-H bond. The dipole moment (units of C·Å) should decrease with a system that more favorably abstracts the aryl H. The dipole moment for $Pd(OAc)_2$ is 1.184 and for $Pd(TFA)_2$ is 1.148, a decrease of 0.04 and a further confirmation that $Pd(TFA)_2$ improves the catalytic efficiency of the CMD mechanism. Thus, the effect of fluorination on the efficiency of the catalysts is clear, since this H-transfer to the fluorinated ligand of Pd(II) is the rate-limiting step of the reaction in the CMD mechanism. This aspect also differs CMD from the other most frequently suspected mechanism, OA, where the rate-determining transition state involves H-transfer to Pd(II) (Fig. 6).

Both **cC** and the preceding transition state, **c1TS**, are more polarised in the case of $Pd(TFA)_2$. The polar solvent,

dichloromethane, used in this reaction further favors these polar structures, lowering the barrier, in agreement with the experiment.

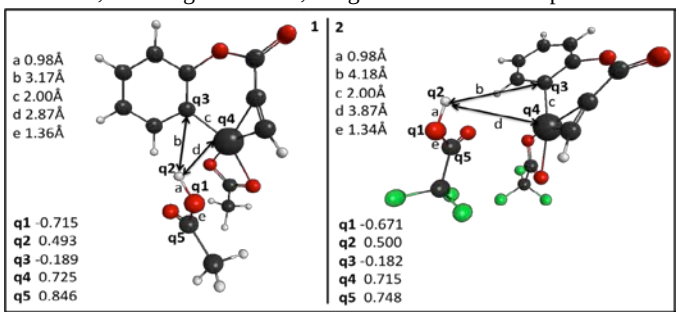

Figure 9. Optimised structures of the Intermediate **cC** in CMD, showing a few characteristic bond lengths and NPA charges on atoms, for 1. the $Pd(OAc)_2$ catalyst, and 2. the $Pd(TFA)_2$ catalyst. The atom colours are black (C), white (N), red (O), and green (F); the large black atom (Pd).

Conclusions

This DFT study shows that the CMD mechanism is preferred in the Pd-catalyzed intramolecular hydroarylation leading to the formation of coumarin. The other alternative mechanisms suggested previously, AMLA, EAS and OA, are suggested to be unfeasible. For AMLA, the possibility of using one acetate for activation of the aryl hydrogen as opposed to two acetates in CMD was tested. It was shown that the AMLA pathway has an exceedingly low TOF, as well as a trapping intermediate along the reaction profile, indicating that AMLA is not a feasible mechanism. For EAS, the *trans*-addition to the ethynyl group (the required first step in electrophilic aromatic substitution) is less energetically favoured than the *cis*-addition form or the intramolecular attachment, which suggests that any mechanism should originate from the *cis*-addition form and immediately discounts EAS as a possible mechanism. For the OA reaction, the cleavage of the aryl C-H on phenylpropiolate has been shown to produce the cationic Pd(II) catalyst strongly bound to the phenylpropiolate, and that does not support the plausibility of the production of the relatively higher energy coumarin product. Coupled with the low approximate TOF value, the OA mechanism is not feasible.

The Pd(II) catalysts with trifluoroacetate (TFA) consistently showed lower barrier heights than that with acetate, in agreement with the experimental results showing greater yields when using TFA. In the case of the CMD mechanism, the dipole moment associated with the abstracted hydrogen and the acetate group oxygen of the $Pd(TFA)_2$ catalyst was shown to decrease, indicating a lower acidity and thus a more favoured hydrogen abstraction with the presence of TFA. The electron-withdrawing effect of TFA causes this improvement in the rate of the reaction. This electron-withdrawing effect leads to the overall greater polarization of the transition state of the rate-determining step on the CMD reaction profile, and of the intermediate following it, leading to their stabilization. A more polar transition state is also favoured in the polar solvent, dichloromethane, which goes in line with the experimentally observed enhanced yield of the reaction in dichloromethane. CMD could be the preferred mechanism for other similar reactions of intramolecular hydroarylation, such as the production of other coumarin and possibly quinilinone compounds.

Acknowledgements

This work was supported by the DARPA Young Faculty Award N66001-11-1-4138. The calculations were carried out on the computers of the Hoffman2 cluster at the Institute for Digital Research and Education (IDRE) located in the University of California, Los Angeles.

Notes and references

[a] Department of Chemistry and Biochemistry, University of California, Los Angeles, CA 90095. E-mail: ana@chem.ucla.edu
[b] California NanoSystems Institute, 570 Westwood Plaza, Building 114, Los Angeles, CA 90095, USA.

† Electronic Supplementary Information (ESI) available: Cartesian coordinates of all stationary state structures in the reaction profiles. See DOI: 10.1039/b000000x/

1. R. F. Heck, *Acc. Chem. Res.* 1979, **12**, 146-151.
2. E. Negishi, A. O. King, N. Okukado, *J. Org. Chem.* 1977, **42**, 1821-1823.
3. C. C. C. Johansson, T. J. Colacot, *Angew Chem Int Edit* 2010, **49**, 676-707.
4. A. E. Shilov, G. B. Shul'pin, *Chem. Rev.* 1997, **97**, 2879-2932.
5. S. Murai, Activation of Unreactive Bonds and Organic Synthesis. In *Topics in organometallic chemistry 3* [Online] Springer,: Berlin ; New York, 1999; p. 272 p. ill. 25 cm. http://uclibs.org/PID/178.
6. Y. Fujiwara, T. Jintoku, K. Takaki, *Chem. Tech.* 1990, **20**, 636-640.
7. G. Dyker, *Angew Chem Int Edit* 1999, **38**, 1699-1712.
8. B. M. Trost, *Science* 1991, **254**, 1471-1477.
9. S. Elnagdy, A. Y. Soliman, H. M. Bakeer, A. M. Youssef, *J. Chem. Soc. Pak.* 1990, **12**, 230-234.
10. B. M. Trost, F. D. Toste, *J. Am. Chem. Soc.* 1996, **118**, 6305-6306.
11. K. Nagasawa, K. Ito, *Heterocycles* 1989, **28**, 703-706.
12. T. Uno, Y. Ozeki, Y. Koga, G. N. Chu, M. Okada, K. Tamura, T. Igawa, F. Unemi, M. Kido, T. Nishi, *Chem Pharm Bull* 1995, **43**, 1724-1733.
13. Z. Y. Yang, Y. Xia, P. Xia, A. Brossi, K. H. Lee, *Tetrahedron Lett.* 1999, **40**, 4505-4506.
14. P. Lopez-Alvarado, C. Avendano, J. C. Menendez, *Synthesis-Stuttgart* 1998, 186-194.
15. A. Arcadi, S. Cacchi, G. Fabrizi, F. Marinelli, P. Pace, *Synlett* 1996, 568.
16. Y. Kitahara, S. Nakahara, M. Shimizu, T. Yonezawa, A. Kubo, *Heterocycles* 1993, **36**, 1909-1924.
17. B. T. Watson, G. E. Christiansen, *Tetrahedron Lett.* 1998, **39**, 9839-9840.
18. K. L. Li, Y. B. Zeng, B. Neuenswander, J. A. Tunge, *J. Org. Chem.* 2005, **70**, 6515-6518.
19. T. Kitamura, K. Otsubo, *J. Org. Chem.* 2012, **77**, 2978-2982.
20. C. Jia, D. Piao, T. Kitamura, Y. Fujiwara, *J. Org. Chem.* 2000, **65**, 7516-7522.
21. J. A. Tunge, L. N. Foresee, *Organometallics* 2005, **24**, 6440-6444.
22. R. H. Crabtree, *The Organometallic Chemistry of the Transition Metals*, 4th ed.; John Wiley: Hoboken, N.J., 2005, p xiii, 546 p.
23. D. Lapointe, K. Fagnou, *Chem. Lett.* 2010, **39**, 1119-1126.
24. C. Engelin, T. Jensen, S. Rodriguez-Rodriguez, P. Fristrup, *Acs Catal* 2013, **3**, 294-302.
25. H. Y. Sun, S. I. Gorelsky, D. R. Stuart, L. C. Campeau, K. Fagnou, *J. Org. Chem.* 2010, **75**, 8180-8189.

26. M. Lafrance, K. Fagnou, *J. Am. Chem. Soc.* 2006, **128**, 16496-16497.
27. M. Lafrance, S. I. Gorelsky, K. Fagnou, *J. Am. Chem. Soc.* 2007, **129**, 14570.
28. Y. Boutadla, D. L. Davies, S. A. Macgregor, A. L. Poblador-Bahamonde, *Dalton T* 2009, 5820-5831.
29. D. L. Davies, S. M. A. Donald, S. A. Macgregor, *J. Am. Chem. Soc.* 2005, **127**, 13754-13755.
30. G. Gerdes, P. Chen, *Organometallics* 2004, **23**, 3031-3036.
31. O. Swang, R. Blom, O. B. Ryan, K. Faegri, *J. Phys. Chem.* 1996, **100**, 17334-17336.
32. T. Yagyu, M. Hamada, K. Osakada, T. Yamamoto, *Organometallics* 2001, **20**, 1087-1101.
33. A. M. LaPointe, M. Brookhart, *Organometallics* 1998, **17**, 1530-1537.
34. S. I. Gorelsky, D. Lapointe, K. Fagnou, *J. Org. Chem.* 2012, **77**, 658-668.
35. R. Ahlrichs, M. Bar, M. Haser, H. Horn, C. Kolmel, *Chem. Phys. Lett.* 1989, **162**, 165-169.
36. K. Eichkorn, O. Treutler, H. Ohm, M. Haser, R. Ahlrichs, *Chem. Phys. Lett.* 1995, **242,** 652-660.
37. C. Hattig, A. Hellweg, A. Kohn, *PCCP* 2006, **8**, 1159-1169.
38. A. Schafer, H. Horn, R. Ahlrichs, *J. Chem. Phys.* 1992, **97**, 2571-2577.
39. J. P. Perdew, J. Tao, V. N. Staroverov, G. E. Scuseria, *J. Chem. Phys.* 2004, **120**, 6898-6911.
40. J. Tao, J. P. Perdew, V. N. Staroverov, G. E. Scuseria, *Phys. Rev. Lett.* 2003, **91**, 146401-1
41. K. P. Jensen *Inorg. Chem.* 2008, **47**, 10357-10365
42. F. Weigend, R. Ahlrichs, *Phys. Chem. Chem. Phys.*, 2005, **7**, 3297–3305
43. S. Grimme, J. Antony, S. Ehrlich, H. Krieg, *J. Chem. Phys.* 2010, **132**.
44. A. E. Reed, R. B. Weinstock, F. Weinhold, *J. Chem. Phys.* 1985, **83**, 735-746.
45. A. Klamt, G. Schuurmann, *J Chem Soc Perk T 2* 1993, 799-805.
46. *Crc Handbook of Chemistry and Physics*, 47th ed.; Sigma-Aldrich.
47. A. Klamt, V. Jonas, *J. Chem. Phys.* 1996, **105**, 9972-9981.
48. S. Kozuch, S. Shaik *Accounts of Chemical Research* 2011, **44**, 101–110

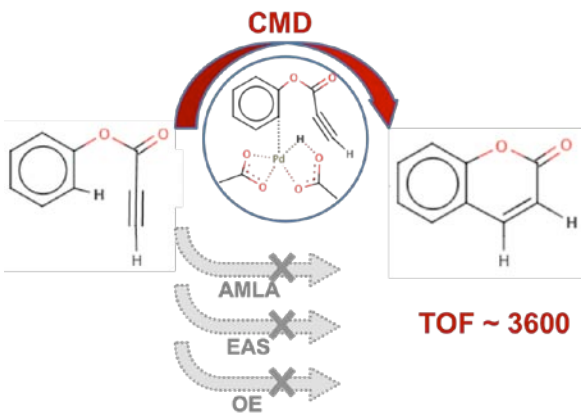

The formation of coumarin via the Pd-catalyzed intramolecular hydroarylation of the C-C triple bond is shown to proceed via concerted metalation-deprotonation (CMD) mechanism.